Cell Tissue Res (2017) 369:527–539
DOI 10.1007/s00441-017-2625-9

REGULAR ARTICLE

MicroRNA-27a/b mediates endothelin-1-induced *PPARγ* reduction and proliferation of pulmonary artery smooth muscle cells

Xinming Xie[1] · Shaojun Li[1] · Yanting Zhu[1] · Lu Liu[1] · Yilin Pan[1] · Jian Wang[1] · Wenhua Shi[1] · Yang Song[1] · Lan Yang[1] · Li Gao[2] · Weijin Zang[3] · Manxiang Li[1]

Received: 30 November 2016 / Accepted: 5 April 2017 / Published online: 8 May 2017
© Springer-Verlag Berlin Heidelberg 2017

Abstract The down-regulation of peroxisome proliferator-activated receptor γ (PPARγ) expression has been found to correlate with the proliferation of pulmonary artery smooth muscle cells (PASMC), pulmonary vascular remodeling and pulmonary hypertension, while the molecular mechanisms underlying *PPARγ* reduction in PASMC remain largely unclear. The aim of the current study is to address this issue. Endothelin-1 (ET-1) dose- and time-dependently resulted in *PPARγ* reduction and proliferation of primary cultured rat PASMC, which was accompanied by the activation of nuclear factor-kappaB (NF-κB) and subsequent induction of microRNA-27a/b (miR-27a/b) expression. Chromatin immunoprecipitation assay revealed that *NF-κB* directly bound to the promoter regions of *miR-27a/b*. Luciferase reporter assay identified that *miR-27a/b* directly regulates the expression of *PPARγ* in PASMC. Further study indicated that the presence of either *NF-κB* inhibitor pyrrolidinedithiocarbamate or prior silencing *miR-27a/b* with anti-miRNA oligonucleotides suppressed ET-1-induced *PPARγ* reduction and proliferation of PASMC, while overexpression of *miR-27a/b* reduced *PPARγ* expression and enhanced PASMC proliferation. Taken together, our study demonstrates that ET-1 stimulates *miR-27a/b* expression by activation of the *NF-κB* pathway, which in turn results in *PPARγ* reduction and contributes to ET-1-induced PASMC proliferation.

Keywords Endothelin-1 · Nuclear factor-kappaB · *miR-27a/b* · Peroxisome proliferator-activated receptor γ · Pulmonary artery smooth muscle cells · Pulmonary hypertension

Abbreviations

BrdU	5-Bromo-29-deoxyuridine
ChIP	Chromatin immunoprecipitation
DMEM	Dulbecco's Modified Eagle Medium
EC	Endothelial cell
EDTA	Ethylene diamine tetraacetic acid
ET-1	Endothelin-1
FBS	Fetal bovine serum
GAPDH	Glyceraldehyde-3-phosphate dehydrogenase
miR	MicroRNA
NC	Negative control
NF-κB	Nuclear factor-kappaB
NP-40	Nonidet P-40
PAECs	Pulmonary arterial endothelial cells
PH	Pulmonary hypertension
PAP	Pulmonary arterial pressure
PASMC	Pulmonary artery smooth muscle cells
PCR	Polymerase chain reaction
PDTC	Pyrrolidine dithiocarbamate
PMSF	Phenylmethylsulfonyl fluoride
PPARγ	Peroxisome proliferator-activated receptor γ
SDS	Sodium dodecyl sulfate
UTR	Untranslated region

✉ Manxiang Li
manxiangli@hotmail.com

[1] Department of Respiratory and Critical Care Medicine, The First Affiliated Hospital of Medical College, Xi'an Jiaotong University, No.277, Yanta West Road, Xi'an, Shaanxi, People's Republic of China 710061

[2] Division of Allergy and Clinical Immunology, Department of Medicine, The Johns Hopkins University School of Medicine, Baltimore, MD 21224, USA

[3] Department of Pharmacology, School of Basic Medical Sciences, Xian Jiaotong University Health Science Center, Xi'an, Shaanxi, People's Republic of China 710061

Introduction

Pulmonary hypertension (PH) is a complex disease characterized by progressive elevation of pulmonary vascular resistance (PVR) and pulmonary artery pressure (PAP) and rapidly leads to right heart failure and death (Bazan and Fares 2015). Despite recent therapeutic advances in the management of PH, its survival rate still remains exceedingly low (Humbert et al. 2010). Different types of PH share a common pathogenesis including vasoconstriction, pulmonary vascular remodeling and thrombosis in situ (Humbert et al. 2004). Vascular remodeling indicates structure changes of the vascular wall and the proliferation of pulmonary artery smooth muscle cell (PASMC) is believed to be critical in this process. However, the molecular mechanisms underlying PASMC proliferation remain largely unclear.

Peroxisome proliferator-activated receptor γ (PPARγ) belongs to the nuclear hormone receptor superfamily. Recent studies have shown that *PPARγ* has broad protective effects on the cardiovascular system beyond its regulation of adipogenesis and glucose metabolism (Fukuda et al. 2015; Gao et al. 2015; Han et al. 2015; Jin et al. 2015b). Further studies have indicated that the reduction of *PPARγ* is found in the pulmonary vasculature of patients with PH (Ameshima et al. 2003). In addition, targeted depletion of *PPARγ* in mice causes spontaneous PH (Guignabert et al. 2009; Hansmann et al. 2008). Several groups including ourselves have reported that activation of *PPARγ* attenuates PASMC proliferation and suppresses the development of PH induced by monocrotaline or hypoxia in rats (Crossno et al. 2007; Kim et al. 2010a; Li et al. 2010; Matsuda et al. 2005; Xie et al. 2015; Zhang et al. 2014). All these suggest that *PPARγ* insufficiency contributes to the development of PH by stimulating PASMC proliferation and pulmonary vascular remodeling. However, the exact mechanisms underlying down-regulation of *PPARγ* in PASMC of PH are still largely unknown.

MicroRNAs (miRNAs) are small non-coding RNA molecules around 22 nucleotides in length and the main function of mature miRNAs is to induce the degradation of mRNA or to suppress its translation (Bartel 2004). Such post-transcriptional regulation is involved in a variety of physiological and pathological cellular processes, including cell proliferation and apoptosis and is also associated with the development of diseases including PH (Brock et al. 2015; Fang and Yeh 2015; Milenkovic 2014; Xing et al. 2015). Recent studies have shown that miRNAs regulate pulmonary vascular remodeling by modulating the proliferation of PASMC (Yang et al. 2012; Zeng et al. 2015). Two miRNA candidates, *miR-27a* and *miR-27b*, are found to target the *PPARγ* 3′ untranslated region (3′ UTR) leading to *PPARγ* down-regulation and to contributing to the proliferation of non-PASMC, including pulmonary artery endothelial cells (PAECs) (Jennewein et al. 2010; Kang et al. 2013; Kim et al. 2010b; Li et al. 2015), while it is unknown whether induction of *miR-27a/b* also mediates the reduction of *PPARγ* expression and is implicated in PASMC proliferation. To examine this, primary cultured PASMC were stimulated with endothelin-1 (ET-1), the expression of *PPARγ* and *miR-27a/b* was determined and the molecular mechanisms underlying these changes were further investigated.

Materials and methods

Cell preparation and culture

Primary PASMC from pulmonary arteries were prepared from Sprague–Dawley rats (70–80 g) according to the method previously described (Ke et al. 2016; Song et al. 2016; Wu et al. 2014). All animal experiments were approved by the Laboratory Animal Care Committee of Xi'an Jiaotong University. All animal care and experiments were performed in accordance with the Guide for the Care and Use of Laboratory Animals of Xi'an Jiaotong University Animal Experiment Center. Briefly, pulmonary arteries were rapidly isolated from sacrificed rats, washed in phosphate-buffered saline (PBS, 4 °C) and dipped into Dulbecco's Modified Eagle Medium (DMEM; Gibco, Grand Isle, NY, USA) containing 10 % fetal bovine serum (FBS; Sijiqing, Hangzhou, China), 100 U/mL penicillin and 100 μg/mL streptomycin. A thin layer of the adventitia was gently stripped off with forceps and the endothelium was carefully removed by scratching the intima surface with elbow tweezers. The remaining smooth muscle was cut into 1-mm^3 pieces and placed into a culture flask and then incubated in a 37 °C, 5 % CO_2 humidified incubator. PASMC were passaged using 0.25 % trypsin (Invitrogen, Carlsbad, CA, USA) until reaching 70–80 % confluence. All experiments were performed with cells between passages 4–6. The purity of the PASMC was determined by immunostaining with α-actin as previously described (Wu et al. 2014).

Cell proliferation assay

Cell proliferation was determined using the BrdU ELISA Kit (Maibio, Shanghai, China) following the established protocol. PASMC were seeded on 96-well plates at 5×10^3 cells per well, allowed to adhere for at least 24 h and then serum-starved overnight (1 % FBS in DMEM) before the start of the experiments. After different treatments, BrdU labeling reagent was added to the wells and incubated for 2 h at 37 °C. Then, the cells were denatured with FixDenat solution for 30 min and incubated with anti-BrdU mAbs conjugated to peroxidase for 90 min at room temperature. After incubation, the antibody conjugate was removed and a substrate solution was added for reaction for 10 min. Finally, the reaction

product was quantified by measuring the absorbance at 370 nm using a microplate reader (Bio-Rad, Richmond, CA, USA). The blank corresponded to 100 μL of culture medium with or without BrdU.

Oligonucleotide synthesis and transfection

For the manual alteration of *miR-27a/b* expression, negative control miRNA (miR-NC), *miR-27a/b* mimics and *miR-27a/b* inhibitor oligonucleotides were purchased from GenePharma (Shanghai, China) and the following sequences were used: *miR-27a* mimics, sense 5′-UUCACAGUGGCUAAGUUCCGC-3′, antisense 5′-GGAACUUAGCCACUGUGAAUU-3′; *miR-27b* mimics, sense 5′-UUCACAGUGGCUAAGUUCUGC-3′, antisense 5′-AGAACUUAGCCACUGUGAAUU-3′; miRNA-NC, sense 5′-UUCUCCGAACGUGUCACGUTT-3′, antisense 5′-ACGUGACACGUUCGGAGAATT-3′; anti-*miR-27a*, 5′-GCGGAACUUAGCCACUGUGAA-3′; anti-*miR-27b*, 5′-GCAGAACUUAGCCACUGUGAA-3′; anti-miRNA-NC, 5′-CAGUACUUUUGUGUAGUACAA-3′. miRNA oligonucleotides were transfected into cultured cells at a final concentration of 50 nM using Lipofectamine™ 2000 reagent (Invitrogen) following the manufacturer's protocols. Briefly, cells were cultured until reaching 30–40 % confluence; miRNA oligonucleotides and Lipofectamine were diluted separately in serum-free DMEM and incubated for 5 min at room temperature. Diluted miRNA oligonucleotides were mixed with diluted Lipofectamine and incubated at room temperature for 20 min. Then, the complex of anti-miRNA and Lipofectamine was added into the cells and they were cultured for the indicated time at 37 °C, 5 % CO_2 in a humidified incubator. The effects of miRNA transfection were analyzed using qRT-PCR.

Quantitative real-time polymerase chain reaction (qRT-PCR)

Total RNA was extracted from PASMC using the RNeasy Micro-plus Kit (Qiagen, Hilden, Germany) following the manufacturer's instructions. Isolated RNAs were polyadenylated using the Thermo Scientific RevertAid First Strand cDNA Synthesis Kit (Logan, UT, USA). The cDNA synthesized was used to perform quantitative PCR on an IQ™5 Real-Time PCR Detection System (Bio-Rad) using the Bio-Rad SsoAdvanced™ Universal SYBR® Green kit. Primers specific for *miR-27a*, *miR-27b*, *U6* small nuclear RNA, *PPARγ* and glyceraldehyde-3-phosphate dehydrogenase (GAPDH) were purchased from Sangon Biotech (Shanghai, China) and the following primer sets were used: rat *miR-27*a, 5′-GTCGTATCCAGTGCAGGGTCCGAGGT ATTCGCACTGGATACGACGCGGAA-3′ (RT primer), 5′-GCGGCG GTTCACAGTGGCTAAG-3′ and 5′-ATCC AGTGCAGGGTCCGAGG-3′; rat *miR-27b*, 5′-GTCGTATCCAGTGCAGGGTCCGAGGTATTCGC ACTGGATACGACGCAGAA-3′ (RT primer), 5′-GCGG CGGTTCACAGTGGCTAAG-3′ and 5′-ATCC AGTGCAGGGTCCGAGG-3′; rat U6, 5′-AACG CTTCACGAATTTGC GTG-3′ (RT primer), 5′-GCTC GCTTCGGCAGCACA-3′ and 5′-GAGGTATTCGCA CCAGAGGA-3′; rat *PPARγ*, 5′-CGGTTGATTTCTCC AGCATT-3′ and 5′-TCGCAC TTTGGTATTCTTGG-3′; rat GAPDH, 5′-CCTGGAGAAACCTGCCAAGTAT-3′ and 5′-CTCGGCCGCCTGCTT-3′. The fold increase relative to control samples was determined by the $2^{-\Delta\Delta Ct}$ method (Livak and Schmittgen 2001). U6 small nuclear RNA served as an internal control for *miR-27a* and *miR-27b*, and GAPDH was used as an internal control for *PPARγ*. Amplification was performed at 95 °C for 1 min, followed by 40 cycles of 95 °C for 5 s, 60 °C for 20 s and 72 °C for 30 s.

Chromatin immunoprecipitation (ChIP) assay

ChIP assay was performed according to the instructions of the EZ-ChIP kit (Millipore, Billerica, MA, USA) as previously described (Au et al. 2013; Jin et al. 2015a; Lv et al. 2016). Briefly, PASMC were treated with formaldehyde and incubated for 10 min to generate DNA-protein cross-links. Cell lysates were then sonicated to generate chromatin fragments of 200–300 bp. The fragmented chromatin samples were immunoprecipitated with antibodies specific for *NF-κB* p65 (Cell Signaling Technology, Danvers, MA, USA) or rabbit control IgG (Millipore) and reverse cross-linked, purified and analyzed using qRT-PCR. The following primer sets were used for the amplicons of the rat *miR-27*a/b promoter regions: *miR-27a* promoter, 5′-CAGGCAGTTGTGACAGTGCT-3′ and 5′-CAGCCAGCTTGGTCTGTGTA-3′; *miR-27*b promoter set 1, 5′-GCAGGTCTTCTTTGCCTGTC-3′ and 5′-CCCAGAACTCCATGCTTTGT-3′; *miR-27*b promoter set 2, 5′-TTGGAGAACAGAGGCACCTT-3′ and 5′-ACAA AGCGGAAACCAATCAC-3′.

Luciferase reporter assay

The wild-type *PPARγ*-3′ UTR (WT) and mutant *PPARγ*-3′ UTR (Mut) containing the putative binding site of *miR-27a/b* were established and cloned in the firefly luciferase expressing vector pMIR-REPORT (Sangon Biotech, Shanghai, China), named as pMIR-*PPARγ*-3′ UTR-WT and pMIR-*PPARγ*-3′ UTR-Mut, respectively. PASMC were seeded into 24-well plates the day before transfection and then co-transfected with 200 ng pMIR-*PPARγ*-3′ UTR-WT or pMIR-*PPARγ*-3′ UTR-Mut reporter vector, 10 pmol *miR-27a/b* mimics or miR-NC and 20 ng renilla luciferase-expressing vector pRL-TK (Promega, Madison, WI, USA) using Lipofectamine 2000 (Invitrogen). After 48 h, cells were harvested and firefly and renilla luciferase activities were measured using the dual-luciferase reporter assay system

(Promega). Luciferase activity of pRL-TK was used as an internal control to normalize transfection and harvest efficiencies. Transfections were performed in triplicate and repeated three times in separate experiments.

Immunoblotting

The cultured cells were washed twice with ice-cold PBS and then lysed in RIPA lysis buffer containing 50 mM Tris-HCl (pH 7.4), 1 % NP-40, 0.1 % SDS, 150 mM NaCl, 0.5 % sodium-deoxycholate, 1 mM EDTA, 1 mM PMSF, 1 mM Na3VO4, 1 mM NaF and proteinase inhibitors. Lysates were centrifuged at 13,000 rpm at 4 °C for 15 min, and the supernatant was collected as total protein. Cytoplasmic and nuclear protein was further extracted using a nuclear and cytoplasmic protein extraction kit (Sangon) according to the manufacturer's instructions. Protein concentration was determined with a BCA protein assay kit (Pierce Biotechnology, Rockford, IL, USA). Protein was separated on a SDS-PAGE gel and transferred to a nitrocellulose (NC; Bio-Rad) membrane via semi-dry transfer. The membrane was then blocked with 5 % (w/v) nonfat dry milk in PBS containing 0.1 % (*v*/v) Tween-20. Polyclonal antibodies against *NF-κB* p65, *PPARγ*, *Lamin B* (Proteintech, Chicago, IL, USA) and glyceraldehyde-3-phosphate dehydrogenase (Chemicon International, Billerica, MA, USA) (1:1000 dilution) were used according to the manufacturer's protocols. Horseradish peroxidase (HRP)-conjugated goat anti-mouse or anti-rabbit IgG was used as the secondary antibodies (Sigma, St. Louis, MO, USA) (1:5000 dilution). Reactions were developed with SuperSignal West Pico Chemiluminescent Substrate (Pierce) and then exposed to the autoradiographic film. Films were scanned and quantified using Quality One software (Bio-Rad).

Statistical analysis

All values were expressed as mean ± standard deviation (S.D.) and analyzed using one-way analysis of variance (ANOVA) with Tukey post hoc test by SPSS13.0 software. Probability values of $P < 0.05$ were considered to represent a statistical significance between groups.

Results

ET-1 stimulates PASMC proliferation

To examine the effect of ET-1 on PASMC proliferation, time-course and dose-response of ET-1 on cell proliferation were investigated. Cell proliferation was determined using a BrdU incorporation assay. As shown in Fig. 1a, ET-1 dose-dependently stimulated PASMC proliferation at 24 h and the maximal BrdU incorporation was a 1.93-fold increase over control

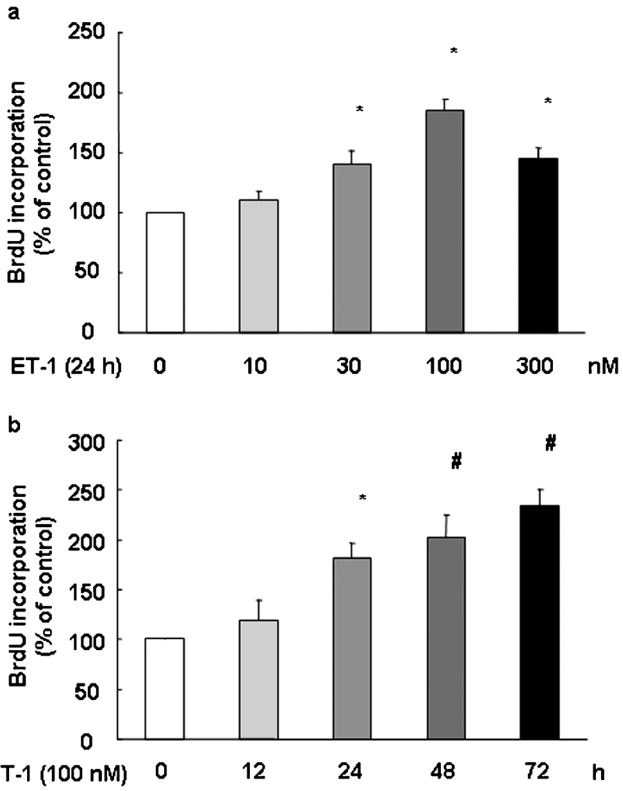

Fig. 1 ET-1 stimulates PASMC proliferation. **a** PASMC were stimulated with different concentrations of ET-1 ranging from 0 to 300 nM for 24 h, and the rate of BrdU incorporation in cells was determined using the BrdU ELISA assay Kit ($n = 4$ each group). **b** Cells were exposed to 100 nM ET-1 for the indicated times, and BrdU incorporation in cells was measured ($n = 4$ each group). *$P < 0.05$ versus control; #$P < 0.01$ versus control

($P < 0.05$) at 100 nM ET-1. Figure 1b demonstrates that ET-1 triggered PASMC proliferation in a time-dependent manner, 100 nM ET-1 caused a significant increase in BrdU incorporation over control after 24 h and BrdU incorporation was a 2.02-fold increase compared to control at 48 h ($P < 0.01$).

ET-1 down-regulates *PPARγ* expression in PASMC

It has been shown that ET-1 down-regulates *PPARγ* expression in several types of non-pulmonary artery smooth muscle cells (Di et al. 2005; Wolf et al. 2014). To clarify whether ET-1 also suppresses *PPARγ* expression in PASMC, cells were treated with different concentrations of ET-1 over different time periods; the expression of *PPARγ* was determined using qRT-PCR and western blotting. As shown in Fig. 2a, ET-1 time-dependently reduced the *PPARγ* mRNA level in PASMC after 24 h treatment, which declined to 0.55-fold over control at 100 nM ET-1 for 48 h incubation ($P < 0.01$ vs. control). Figure 2b shows the time course of 100 nM ET-1 regulation of the *PPARγ* protein level, which dropped to 0.48-fold compared to control at 48 h ($P < 0.01$). Figure 2c, d indicates that ET-1

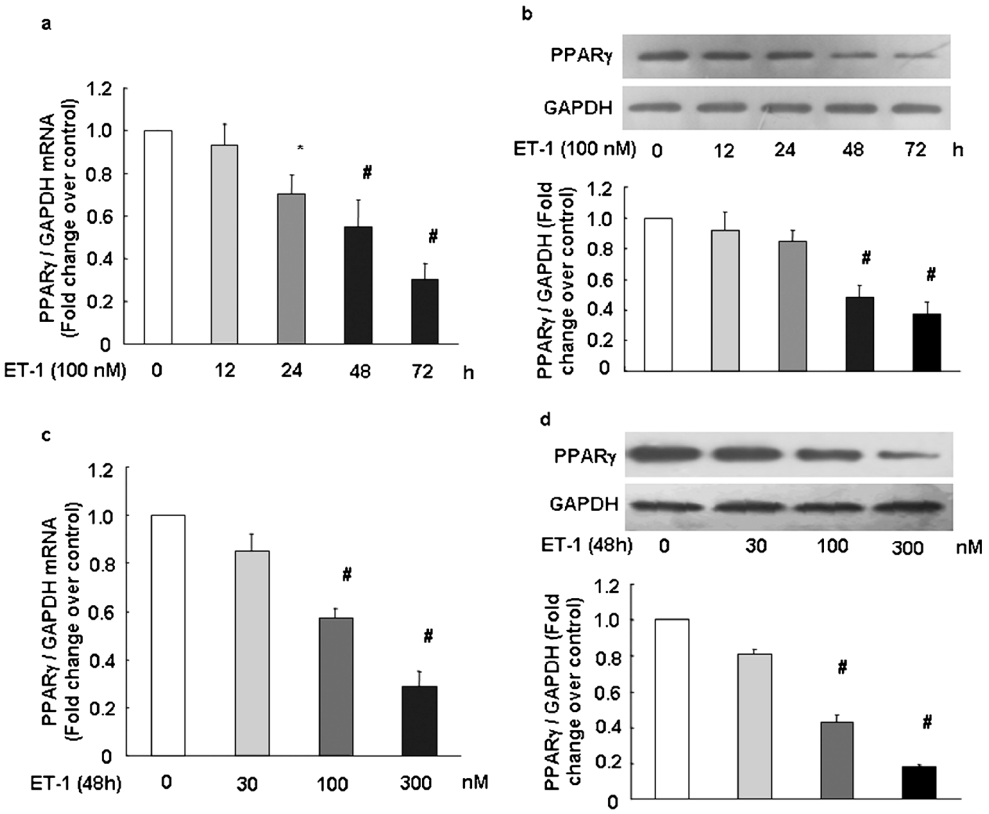

Fig. 2 ET-1 time-and dose-dependently reduces *PPARγ* expression in PASMC. Cells were treated with 100 nM ET-1 for the indicated times and the levels of *PPARγ* **a** mRNA and **b** protein were determined using RT-PCR and immunoblotting ($n = 4$ each group). Cells were stimulated with different concentrations of ET-1 ranging from 0 to 300 nM for 48 h and the levels of *PPARγ* **c** mRNA and **d** protein were determined using qRT-PCR and immunoblotting ($n = 4$ each group). *$P < 0.05$ versus control and #$P < 0.01$ versus control

down-regulated *PPARγ* expression in PASMC in a dose-dependent manner at 48 h and 100 nM ET-1 reduced *PPARγ* mRNA and protein levels to 0.57-fold and 0.43-fold compared to control, respectively (both $P < 0.01$). These results suggest that ET-1 also suppresses *PPARγ* expression in PASMC.

Activation of *NF-κB* signaling mediates ET-1-induced *PPARγ* reduction in PASMC

To address the molecular mechanisms underlying ET-1-induced *PPARγ* reduction in PASMC, cells were treated with 100 nM ET-1 for 48 h with or without pre-incubation of cells with selective *NF-κB* inhibitor PDTC (50 μM) for 2 h and then the translocation of the p65 subunit of *NF-κB* from cytosol to nucleus was examined using western blotting. As shown in Fig. 3a, treatment of PASMC with 100 nM ET-1 for 48 h resulted in a 3.30-fold increase in the p65 subunit nuclear translocation compared to control ($P < 0.01$), while pre-treatment of cells with PDTC ameliorated ET-1-induced p65 nuclear translocation, which declined to a 2.10-fold increase over control ($P < 0.01$ vs. ET-1-treated cells). At the same time, the p65 protein level in the cytosol was increased from 0.65-fold over control in ET-1-treated cells to 0.93-fold over control in PDTC and ET-1 co-treated cells ($P < 0.01$) (Fig. 3a).

To investigate the specific involvement of the *NF-κB* pathway in ET-1-induced *PPARγ* reduction, primary cultured PASMC were prior incubated with *NF-κB* inhibitor PDTC (50 μM) for 2 h, followed by stimulation with 100 nM ET-1 for 48 h and then the mRNA and protein levels of *PPARγ* were determined. The presence of PDTC dramatically blocked ET-1 reduction of *PPARγ* mRNA and protein levels, which increased from 0.51-fold and 0.43-fold over control in ET-1-treated cells to 0.80-fold and 0.88-fold over control in cells simultaneously treated with PDTC and ET-1, respectively (both $P < 0.01$) (Fig. 3b, c). These results indicate that activation of *NF-κB* particularly mediates ET-1 down-regulation of *PPARγ* expression in PASMC.

NF-κB mediates ET-1 up-regulation of *miR-27a/b* in PASMC

Previous studies have reported that *PPARγ* is regulated by *miR-27a/b* in several types of cells (Jennewein et al. 2010; Kang et al. 2013; Kim et al. 2010b; Li et al. 2015). At the same time, the level of *miR-27* is increased in the lung tissue of several experimental models of PH (Bi et al. 2015; Caruso et al. 2010; Kang et al. 2013) and in hypoxia-exposed human pulmonary artery endothelial cells (Kang et al. 2013). A variety of studies have found that several microRNAs, including *miR-27a/b*, are directly regulated by *NF-κB* and are associated with

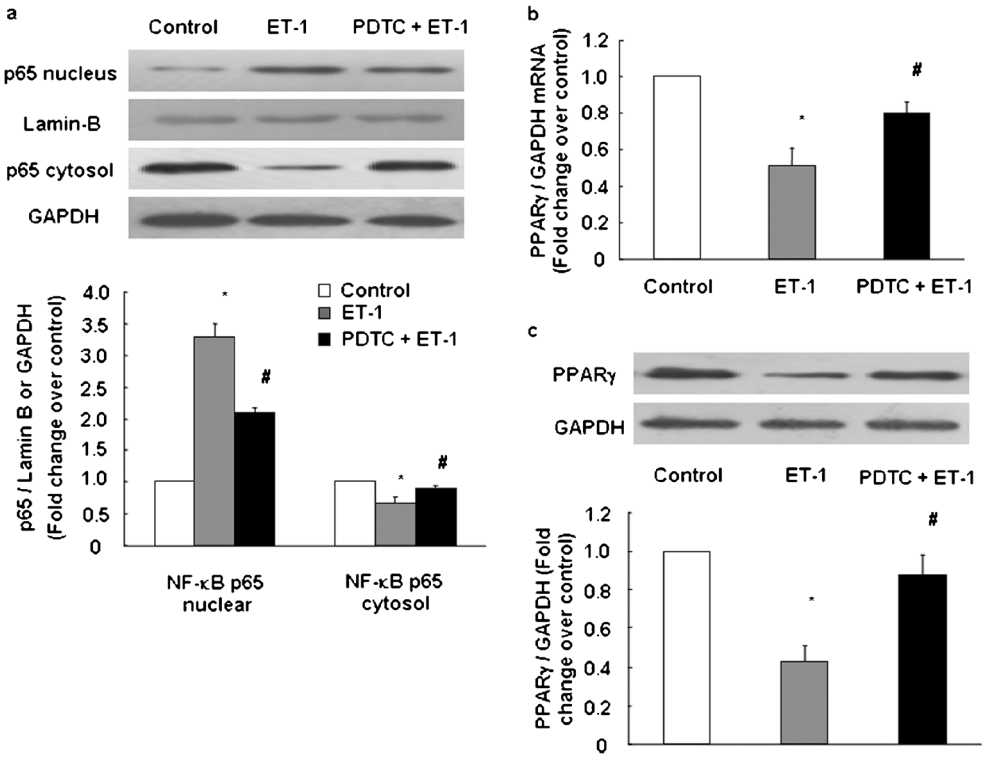

Fig. 3 *NF-κB* mediates ET-1-induced *PPARγ* reduction in PASMC. **a** Cells were pretreated with or without *NF-κB* inhibitor PDTC (50 μM) for 2 h before stimulation with ET-1 (100 nM) for 48 h. Then the protein level of the *NF-κB* p65 subunit in the cytoplasmic and nuclear fraction was determined using western blot and *Lamin B* and GAPDH served as loading control for the nuclear and cytoplasmic protein, respectively ($n = 4$ each group). **b** Level of *PPARγ* mRNA was determined using qRT-PCR, and GAPDH served as an internal control ($n = 4$ each group). **c** *PPARγ* protein level was determined using immunoblotting ($n = 4$ each group). *$P < 0.01$ versus control and #$P < 0.01$ versus ET-1-treated cells

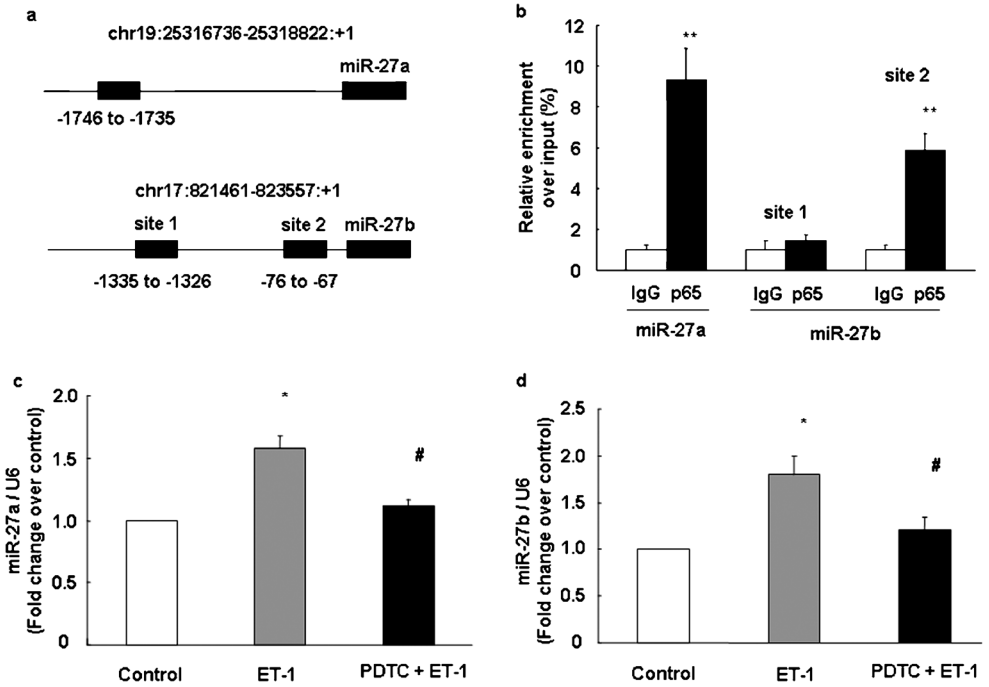

Fig. 4 *NF-κB* mediates ET-1-induced *miR-27a/b* up-regulation through direct binding to its promoter regions in PASMC. **a** Schematic representation of the intact *NF-κB* binding site within the *miR-27a/b* promoters. **b** ChIP assay coupled with qRT-PCR analysis reveals the relative enrichment of *NF-κB* p65 on the *miR-27*a/b promoters in PASMC after stimulation with ET-1 (100 nM) for 48 h. Fold of enrichment of ChIP assay was calculated with reference to control IgG after normalized with the input DNA ($n = 4$ each group). Cells were prior treated with or without an inhibitor of *NF-κB* PDTC (50 μM) for 2 h, followed by stimulation with ET-1(100 nM) for 48 h. The levels of **c** *miR-27*a and **d** *miR-27*b were measured using qRT-PCR. U6 small nuclear RNA served as a loading control ($n = 4$ each group). *$P < 0.05$ versus control, **$P < 0.01$ versus IgG and #$P < 0.05$ versus ET-1-treated cells

multiple physiological and pathophysiological processes (Fiorillo et al. 2015; Zhu et al. 2014). Therefore, it is interesting to know whether *NF-κB* mediates ET-1 induction of *miR-27a/b* expression in PASMC.

To test this hypothesis, the genomic sequences of rat *miR-27*a/b were obtained from the online database (http://www.genome.ucsc.edu) and the potential *NF-κB* binding sites in the promoter regions of *miR-27*a/b were analyzed using the PROMO database (http://alggen.lsi.upc.es/cgi-bin/promo_v3/promo/promo.cgi?dirDB=TF_8.3). The results revealed that there was one binding site in the promoter region (−1746 to −1735) of rat *miR-27*a and two were found within the *miR-27*b promoter region and named as set 1 (−1335 to −1326) and set 2 (−76 to −67), respectively (Fig. 4a). To further validate that *NF-κB* can directly bind to the *miR-27a/b* promoter regions, ChIP assays were used to examine whether *NF-κB* directly bound to putative sites identified in the *miR-27a/b* promoters after treatment with ET-1 (100 nM) for 48 h. Our results indicated that enrichment of *NF-κB* p65 was observed around the promoter region (−1746 to −1735) of *miR-27a* and set 2 (−76 to −67) of *miR-27b* compared with the control IgG (both $P < 0.01$) (Fig. 4b). These results suggest that *NF-κB* can bind to the promoter regions of *miR-27*a/b in PASMC.

To confirm that *NF-κB* directly mediates ET-1-induced *miR-27*a/b expression in PASMC, cells were pretreated with *NF-κB* inhibitor PDTC (50 μM) for 2 h before stimulation of cells with 100 nM ET-1 for 48 h. As shown in Fig. 4c, d, PASMC treated with ET-1(100 nM) for 48 h exhibited a 1.58-fold and 1.79-fold increase over control in the levels of *miR-27a* and *miR-27b*, respectively (both $P < 0.05$), while pre-incubation of cells with *NF-κB* inhibitor PDTC (50 μM) for 2 h reduced the levels of *miR-27a* and *miR-27b* to 1.12-fold and 1.15-fold over control, respectively (both $P < 0.05$ versus ET-1-treated cells). These results suggest that the *NF-κB* pathway is specifically involved in ET-1 up-regulation of *miR-27a/b* through direct binding to its promoters in PASMC.

PPARγ is a direct target of *miR-27a/b* in PASMC

In order to determine whether *miR-27a/b* directly binds to 3′ UTR of *PPARγ* mRNA and regulates its expression in PASMC, we performed a luciferase assay in pMIR-*PPARγ*-3′ UTR-WT or pMIR-*PPARγ*-3′ UTR-Mut luciferase reporter plasmids transfected into PASMC. In pMIR-*PPARγ*-3′ UTR-Mut, four nucleotides were changed to disrupt the putative interaction between *PPARγ* mRNA and *miR-27a/b* (Fig. 5a). As shown in Fig. 5b, co-transfection of *miR-27a* or *miR-27b* with pMIR-*PPARγ*-3′ UTR-WT significantly suppressed the luciferase activity in PASMC, which declined to 0.62-fold and 0.56-fold compared with miR-NC transfected cells, respectively (both $P < 0.01$). In contrast, co-transfection of *miR-27a/b* or miR-NC with pMIR-*PPARγ*-3′ UTR-Mut did not affect the luciferase activity in PASMC. These results suggest that *PPARγ* is a direct target of *miR-27a/b* in PASMC.

Next, we determined the effect of overexpression or down-regulation of *miR-27a/b* on *PPARγ* expression in PASMC. As shown in Fig. 5c, transfection of 50 nM *miR-27a* or *miR-27b* mimics for 48 h reduced the *PPARγ* mRNA level to 0.53-fold and 0.49-fold compared with miR-NC transfected cells, respectively (both $P < 0.01$). Meanwhile, the *PPARγ* protein level was also decreased to 0.45-fold and 0.40-fold compared with miR-NC transfected cells, respectively (both $P < 0.01$) (Fig. 5d). In contrast, in PASMC transfected with 50 nM anti-*miR-27a* or anti-*miR-27b* oligonucleotides for 48 h, the *PPARγ* protein levels were significantly increased to 2.66-fold and 2.80-fold compared with anti-miR-NC transfected cells, respectively (both $P < 0.01$) (Fig. 5e).

To further examine whether *miR-27a/b* specifically mediates ET-1-induced *PPARγ* reduction in PASMC, we applied sequence-specific anti-miRNA to knockdown the expression of *miR-27a/b*. As shown in Fig. 6a, transfection of PASMC with anti-*miR-27a* or anti-*miR-27b* for 48 h resulted in 67 % and 62 % reduction in *miR-27a* and *miR-27b* levels compared to control, respectively (both $P < 0.01$), whereas anti-miR-NC transfection did not change the *miR-27a/b* level. Figure 6b indicates that treatment of PASMC with 100 nM ET-1 for 48 h reduced the *PPARγ* mRNA level to 0.50-fold over control ($P < 0.01$), whereas the *PPARγ* mRNA level raised to 0.69-fold and 0.85-fold compared to control in cells prior transfected with anti-*miR-27a* or anti-*miR-27b* for 24 h and then followed by ET-1 stimulation for 48 h, respectively (both $P < 0.05$ vs. ET-1-treated cells). Similarly, lacking *miR-27a* or *miR-27b* also suppressed ET-1-induced *PPARγ* protein reduction in PASMC. The protein level of *PPARγ* raised from 0.46-fold over control in ET-1-treated cells to 0.74-fold and 0.91-fold increase over control in cells with prior transfection of anti-*miR-27a* or anti-*miR-27b*, respectively (both $P < 0.05$ vs. ET-1-treated cells) (Fig. 6c). Taken together, these results suggest that *miR-27a/b* directly regulates *PPARγ* expression and mediates ET-1-induced *PPARγ* down-regulation in PASMC.

Up-regulation of *miR-27a/b* by *NF-κB* mediates ET-1-stimulated PASMC proliferation

To determine the effect of overexpression of *miR-27a/b* on PASMC proliferation, PASMC were transfected with 50 nM *miR-27a/b* mimics or miR-NC for 48 h. Figure 7a demonstrates that the rate of BrdU incorporation increased to 1.75-fold and 1.89-fold over control in cells transfected with *miR-27a* or *miR-27b* mimics, respectively (both $P < 0.01$ vs. miR-NC transfected cells). To further clarify whether up-regulation of *miR-27a/b* by *NF-κB* activation and subsequent *PPARγ* reduction are involved in ET-1-stimulated PASMC proliferation, cells were pre-incubated with PDTC (50 μM) for 2 h, or prior transfected with 50 nM anti-*miR-27a* or anti-*miR-27b* oligonucleotides for 24 h, followed by 100 nM ET-1 stimulation for 48 h. PASMC

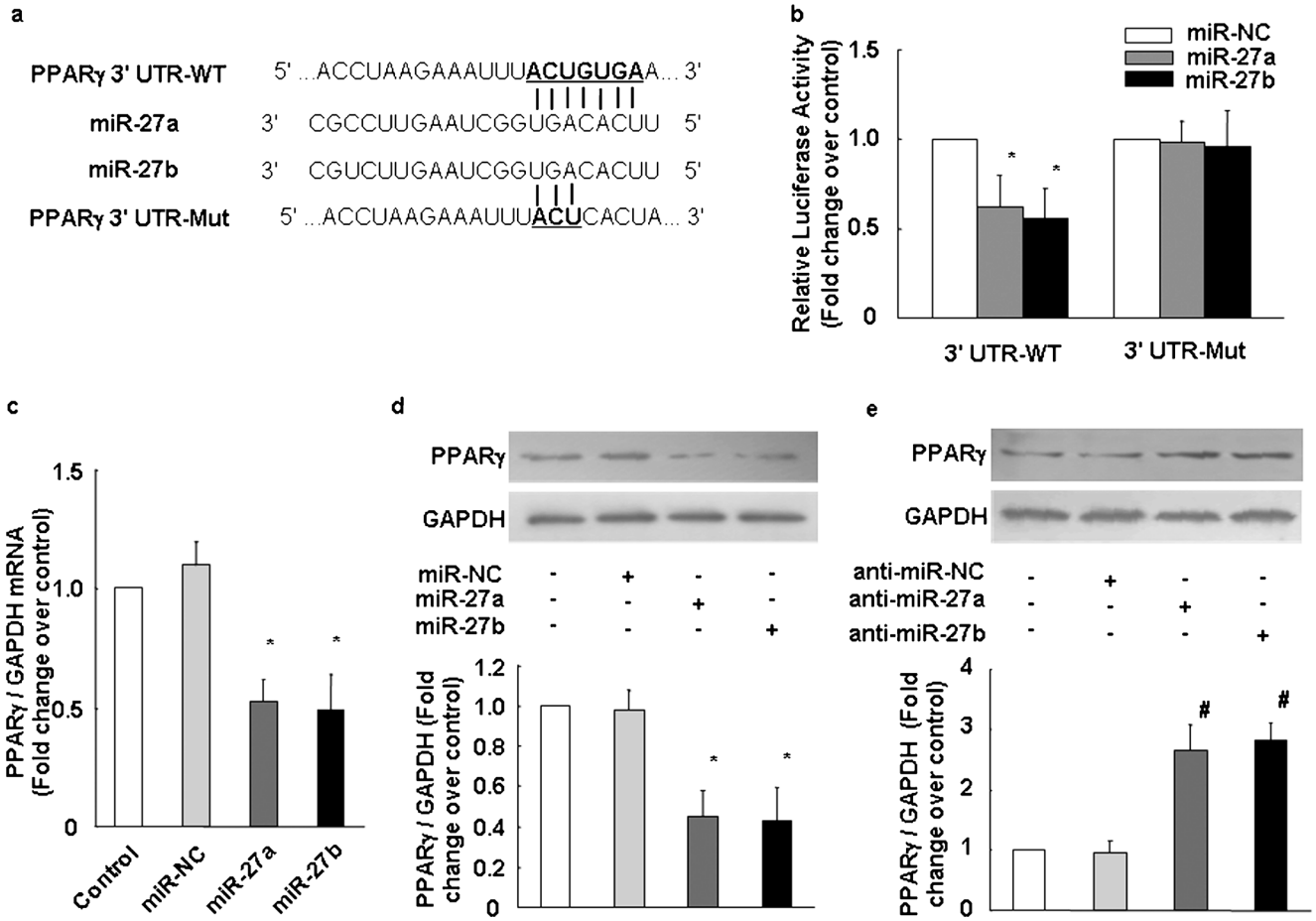

Fig. 5 *PPARγ* is a direct target of *miR-27a/b* in PASMC. **a** Schematic of *miR-27a/b* target sequence in 3′ UTR of *PPARγ* and its mutated version. **b** pMIR-*PPARγ*-3′ UTR-WT or pMIR-*PPARγ*-3′ UTR-Mut reporter vector, *miR-27a/b* mimics or miR-NC and pRL-TK vector were co-transfected into PASMC and a luciferase assay was performed 48 h after transfection (n = 3 each group). **c** qRT-PCR analysis of *PPARγ* mRNA expression after *miR-27a/b* mimics transfection for 48 h in PASMC (n = 3 each group). **d**, **e** Western blot analysis of *PPARγ* protein expression after 50 nM *miR-27a/b* mimics, or anti-*miR-27a/b* oligonucleotides transfection for 48 h in PASMC (n = 3 each group). *$P < 0.01$ versus miR-NC transfected cells and #$P < 0.01$ versus anti-miR-NC transfected cells

proliferation was determined by BrdU incorporation assay. As shown in Fig. 7b, inhibition of *NF-κB* dramatically suppressed ET-1-triggered PASMC proliferation, the BrdU incorporation rate was decreased from a 2.12-fold increase over control in ET-1-treated cells to a 1.20-fold increase over control in PDTC and ET-1 co-treated cells ($P < 0.01$). In addition, the rate of BrdU incorporation declined from 1.98-fold over control in ET-1 treated cells with prior transfection of anti-miR-NC to 1.53-fold and 1.30-fold over control in ET-1 treated cells with prior transfection of anti-*miR-27a* or anti-*miR-27b*, respectively ($P < 0.05$). These results suggest that up-regulation of *miR-27a/b*, especially *miR-27b*, by *NF-κB* activation mediates the effect of ET-1 on PASMC proliferation.

Discussion

We have shown in this study that ET-1 causes the reduction of *PPARγ* expression in primary cultured PASMC, this effect is coupled to ET-1-induced *NF-κB* activation and subsequent induction of *miR-27a/b*, particularly *miR-27b*, which further post-transcriptional suppresses the expression of *PPARγ* and regulates the proliferation of PASMC. Our study provides molecular mechanisms underlying the reduction of *PPARγ* in pulmonary vasculature in the development of PH.

Insufficiency of *PPARγ* function due to its protein level reduction has been shown to be associated with the development of a variety of diseases including various types of cancer (Chang et al. 2006; Mansure et al. 2013; Pellerito et al. 2014) and activation of *PPARγ* suppresses both normal and tumor cell proliferation (Kollipara and Kittler 2015; Luo et al. 2015; Zhang et al. 2015). Recent studies have further indicated that a reduction of *PPARγ* expression has been observed in the vascular lesions of patients with PH and several experimental models of PH (Ameshima et al. 2003; Bijli et al. 2015; Green et al. 2012; Kang et al. 2013; Kim et al. 2010a; Lu et al. 2013). Activation of *PPARγ* with exogenous synthetic thiazolidinedione ligands attenuates pulmonary vascular

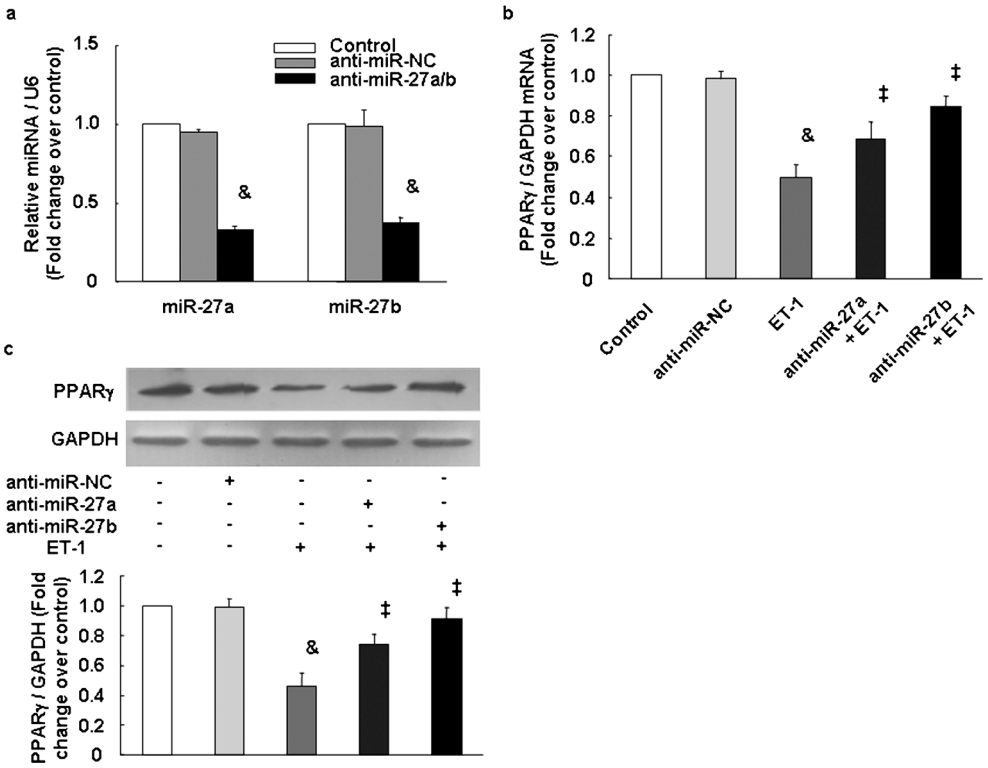

Fig. 6 Inhibition of *miR-27a/b* suppresses ET-1-induced *PPARγ* reduction in PASMC. **a** The expression of *miR-27a/b* was examined by qRT-PCR in cells transfected with or without indicated anti-miRNA oligonucleotides for 48 h ($n = 4$ each group). PASMC were prior transfected with anti-*miR-27*a or anti-*miR-27*b for 24 h and then followed by ET-1 stimulation for 48 h, *PPARγ* **b** mRNA and **c** protein expressions were analyzed using real-time PCR and western blot analysis ($n = 4$ each group). &$P < 0.01$ versus anti-miR-NC and ‡$P < 0.05$ versus ET-1-treated cells

remodeling and therefore the development of PH by inhibiting PASMC proliferation in several experimental models of PH (Gien et al. 2014; Kang et al. 2013; Liu et al. 2012. 2014; Xie et al. 2015; Zhang et al. 2014). The finding of an association between *PPARγ* and the development of PH have brought new perspectives for understanding and treatment of this disease, while the detailed molecular mechanisms responsible for the reduction of *PPARγ* in pulmonary vasculature of PH remain largely unknown. It has been shown that exogenous ET-1 administration decreases *PPARγ* expression in pulmonary artery endothelial cells (Wolf et al. 2014) and aortic vascular smooth muscle cells (Di et al. 2005). Increased level of plasma ET-1 has also been found in patients with PH and animal models of PH (Kojonazarov et al. 2012; Kwon et al. 2010; Stewart et al. 1991; Yuan et al. 2013; Zhang et al. 2005). In addition, previous studies have shown that the plasma ET-1 level predicts disease severity and degree of PH in newborn lambs and human infants with persistent PH of the newborn (de Vroomen et al. 2001; Keller et al. 2010). In the present study, we demonstrated that ET-1 dose- and time-dependently reduced *PPARγ* expression and stimulated PASMC proliferation. Although it is hard to correlate the biological relevance of ET-1 level in vivo versus in vitro, these results suggest that ET-1-induced *PPARγ* reduction might play an important role in the development of PH.

NF-κB is a transcriptional factor that regulates multiple genes expression associated with cellular proliferation, differentiation inflammation and angiogenesis (Monaco et al. 2004). *NF-κB* can be activated by a variety of stimuli, such as hypoxia, inflammatory cytokines, viral and bacterial infections, and oxidative and DNA-damaging agents (Ghosh and Karin 2002). The activation of the *NF-κB* pathway requires the release of p65/p50 subunits from the complex with the inhibitor of κB and the translocation of p65/p50 heterodimers to the nucleus (Rahman and Fazal 2011). Previous studies have indicated that PASMC derived from patients with idiopathic pulmonary arterial hypertension show an increased *NF-κB* activity and inhibition of *NF-κB* ameliorates the development of PH in several experimental models (Hosokawa et al. 2013; Huang et al. 2008; Li et al. 2014; Sawada et al. 2007). A study by Lu et al. showed that hypoxia-induced activation of *NF-κB* reduces *PPARγ* expression and promotes PASMC proliferation; knockdown of *NF-κB* in PASMC can reverse hypoxic-induced *PPARγ* reduction and cell proliferation (Lu et al. 2013). In this study, we further indicated that ET-1 also activated *NF-κB* cascade and caused *PPARγ* downregulation and pharmacological inhibition of *NF-κB* by PDTC abolished ET-1-induced *PPARγ* reduction and therefore suppressed PASMC proliferation. In addition, reduction of *PPARγ* has been shown to be sufficient to induce the activation of *NF-κB* in human PASMC, suggesting the presence of feed-forward or self-amplifying signaling mechanisms in PASMC (Bijli et al. 2015). Actually, there is an interaction loop between *NF-κB* and *PPARγ* (Kelly et al. 2004) activation of *PPARγ* suppresses the activity of *NF-κB* and inhibits its caused pathological alterations, such as cell proliferation

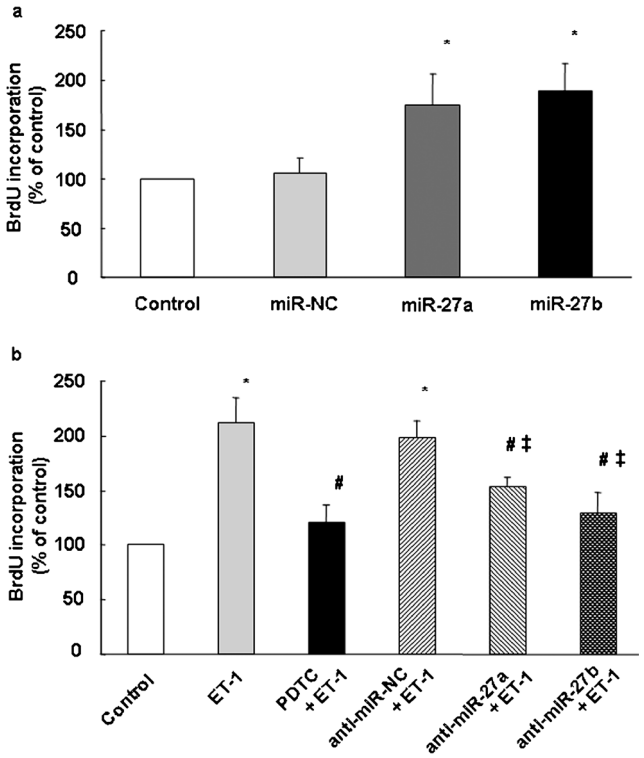

Fig. 7 *NF-κB*-dependent *miR-27a/b* up-regulation mediates ET-1-induced PASMC proliferation. **a** PASMC were transfected with 50 nM miR-NC or *miR-27a/b* mimics for 48 h, and cell proliferation was measured using BrdU incorporation assay ($n = 4$ each group). **b** PASMC were pre-incubated with an inhibitor of *NF-κB* PDTC (50 μM) for 2 h, or pre-transfected with 50 nM indicated anti-miRNA oligonucleotides for 24 h and then stimulated with100 nM ET-1 for 48 h. BrdU incorporation was measured in cells ($n = 4$ each group). $^*P < 0.01$ versus control, $\#P < 0.05$ versus ET-1-treated cells and $\ddagger P < 0.05$ versus anti-miR-NC with ET-1

and inflammatory responses (Ackerman et al. 2005; Ban et al. 2011; Lu et al. 2010). Our present study and others suggest that *NF-κB* not only induces particular pathophysiological changes but also amplifies its effects by blocking its intrinsic inhibitors, such as *PPARγ* (Bijli et al. 2015; Liu et al. 2011; Lu et al. 2013).

miR-27a/b is a member of homologous miRNA clusters, *miR-23a/27a/24–2* and *23b/27b/24–1*, which are found on human chromosomes 19 and 9, respectively. They have the same sequence, UGACACU, which recognizes its complementary sequence in the 3′ UTRs of specific genes, including *PPARγ* (Lin et al. 2009). Previous studies suggest that *miR-27a/b* has profound effects on cell proliferation, differentiation and survival (Chintharlapalli et al. 2009; Lin et al. 2009; Liu et al. 2009; Zhu et al. 2008). *miR-27* is increased in the lung tissue of several experimental models of PH (Bi et al. 2015; Caruso et al. 2010) and in hypoxia-exposed human pulmonary artery endothelial cells (Kang et al. 2013). It is widely recognized that structural alterations in the vascular wall contribute to all forms of PH and PAECs injury and dysfunction, as well as PASMC proliferation and migration, are strongly suspected to be key contributing factors in initiating and mediating pulmonary vascular remodeling in PH (Kang et al. 2013; Zeng et al. 2015). The study by Kang et al. showed that hypoxia inhibits *PPARγ* expression and promotes human PAECs proliferation through *miR-27a*-mediated post-transcriptional mechanisms (Kang et al. 2013). A recent study showed that *miR-27b* affects NO production via the modulation of *PPARγ* expression in human PAECs and that *miR-27b* inhibition attenuates pulmonary vascular remodeling and prevents right ventricular hypertrophy in monocrotaline-induced PH in rats (Bi et al. 2015). However, the detailed molecular mechanisms responsible for *miR-27* induction of pulmonary vascular remodeling, particularly PASMC proliferation, remain unclear. In this study, ChIP assays indicated that *NF-κB* directly bind to the miR-27a/b promoter regions. The use of an *NF-κB* inhibitor further confirmed that activation of *NF-κB* mediated ET-1-induced miR-27a/b expression and up-regulation of *miR-27*, particularly *miR-27b*, in turn reduced *PPARγ* expression and contributed to ET-1-induced PASMC proliferation. Further studies are needed to explore whether these mechanisms play a role in the development of a variety of PH in vivo. Nevertheless, this study provides molecular insights into *PPARγ* down-regulation in PH and has a potential value in the treatment of PH.

Acknowledgement This study was supported by the National Natural Science Foundation of China (Grant No. 81070045).

Compliance with ethical standards The funders of this project had no role in the study design, data collection and analysis, decision to publish, or preparation of the manuscript.

Competing interests The authors have declared no conflict of interest.

References

Ackerman WET, Zhang XL, Rovin BH, Kniss DA (2005) Modulation of cytokine-induced cyclooxygenase 2 expression by PPARG ligands through NFkappaB signal disruption in human WISH and amnion cells. Biol Reprod 73:527–535

Ameshima S, Golpon H, Cool CD, Chan D, Vandivier RW, Gardai SJ, Wick M, Nemenoff RA, Geraci MW, Voelkel NF (2003) Peroxisome proliferator-activated receptor gamma (PPARgamma) expression is decreased in pulmonary hypertension and affects endothelial cell growth. Circ Res 92:1162–1169

Au SL, Wong CC, Lee JM, Wong CM, Ng IO (2013) EZH2-mediated H3K27me3 is involved in epigenetic repression of deleted in liver cancer 1 in human cancers. PLoS ONE 8:e68226

Ban JO, Oh JH, Son SM, Won D, Song HS, Han SB, Moon DC, Kang KW, Song MJ, Hong JT (2011) Troglitazone, a PPAR agonist, inhibits human prostate cancer cell growth through inactivation of NFkappaB via suppression of GSK-3beta expression. Cancer Biol Ther 12:288–296

Bartel DP (2004) MicroRNAs: genomics, biogenesis, mechanism, and function. Cell 116:281–297

Bazan IS, Fares WH (2015) Pulmonary hypertension: diagnostic and therapeutic challenges. Ther Clin Risk Manag 11:1221–1233

Bi R, Bao C, Jiang L, Liu H, Yang Y, Mei J, Ding F (2015) MicroRNA-27b plays a role in pulmonary arterial hypertension by modulating peroxisome proliferator-activated receptor gamma dependent Hsp90-eNOS signaling and nitric oxide production. Biochem Biophys Res Commun 460:469–475

Bijli KM, Kleinhenz JM, Murphy TC, Kang BY, Adesina SE, Sutliff RL, Hart CM (2015) Peroxisome proliferator-activated receptor gamma depletion stimulates Nox4 expression and human pulmonary artery smooth muscle cell proliferation. Free Radic Biol Med 80:111–120

Brock M, Haider TJ, Vogel J, Gassmann M, Speich R, Trenkmann M, Ulrich S, Kohler M, Huber LC (2015) The hypoxia-induced microRNA-130a controls pulmonary smooth muscle cell proliferation by directly targeting CDKN1A. Int J Biochem Cell Biol 61: 129–137

Caruso P, MacLean MR, Khanin R, McClure J, Soon E, Southgate M, MacDonald RA, Greig JA, Robertson KE, Masson R, Denby L, Dempsie Y, Long L, Morrell NW, Baker AH (2010) Dynamic changes in lung microRNA profiles during the development of pulmonary hypertension due to chronic hypoxia and monocrotaline. Arterioscler Thromb Vasc Biol 30:716–723

Chang AJ, Song DH, Wolfe MM (2006) Attenuation of peroxisome proliferator-activated receptor gamma (PPARgamma) mediates gastrin-stimulated colorectal cancer cell proliferation. J Biol Chem 281:14700–14710

Chintharlapalli S, Papineni S, Abdelrahim M, Abudayyeh A, Jutooru I, Chadalapaka G, Wu F, Mertens-Talcott S, Vanderlaag K, Cho SD, Smith R 3rd, Safe S (2009) Oncogenic microRNA-27a is a target for anticancer agent methyl 2-cyano-3,11-dioxo-18beta-olean-1,12-dien-30-oate in colon cancer cells. Int J Cancer 125:1965–1974

Crossno JT Jr, Garat CV, Reusch JE, Morris KG, Dempsey EC, McMurtry IF, Stenmark KR, Klemm DJ (2007) Rosiglitazone attenuates hypoxia-induced pulmonary arterial remodeling. Am J Physiol Lung Cell Mol Physiol 292:L885–L897

de Vroomen M, Lopes Cardozo RH, Steendijk P, Frolich M, Baan J, van Bel F (2001) Endothelin-1 plasma concentration increases in the early phase of pulmonary hypertension development during respiratory distress syndrome: a study in newborn lambs. Early Hum Dev 63:9–21

Di ZL, Niu XL, Wei J, Gao DF, Wang NP (2005) Effect of endothelin-1 stimulation on peroxisome proliferator-activated receptor-gamma expression in vascular smooth muscle cells. Di Yi Jun Yi Da Xue Xue Bao 25:1140–1144

Fang YC, Yeh CH (2015) Role of microRNAs in vascular remodeling. Curr Mol Med 15:684–696

Fiorillo AA, Heier CR, Novak JS, Tully CB, Brown KJ, Uaesoontrachoon K, Vila MC, Ngheim PP, Bello L, Kornegay JN, Angelini C, Partridge TA, Nagaraju K, Hoffman EP (2015) TNF-alpha-induced microRNAs control dystrophin expression in Becker muscular dystrophy. Cell Rep 12:1678–1690

Fukuda K, Matsumura T, Senokuchi T, Ishii N, Kinoshita H, Yamada S, Murakami S, Nakao S, Motoshima H, Kondo T, Kukidome D, Kawasaki S, Kawada T, Nishikawa T, Araki E (2015) Statins meditate anti-atherosclerotic action in smooth muscle cells by peroxisome proliferator-activated receptor-gamma activation. Biochem Biophys Res Commun 457:23–30

Gao D, Hao G, Meng Z, Ning N, Yang G, Liu Z, Dong X, Niu X (2015) Rosiglitzone suppresses angiotensin II-induced production of KLF5 and cell proliferation in rat vascular smooth muscle cells. PLoS ONE 10:e0123724

Ghosh S, Karin M (2002) Missing pieces in the NF-kappaB puzzle. Cell 109(Suppl):S81–S96

Gien J, Tseng N, Seedorf G, Roe G, Abman SH (2014) Peroxisome proliferator activated receptor-gamma-rho-kinase interactions contribute to vascular remodeling after chronic intrauterine pulmonary hypertension. Am J Physiol Lung Cell Mol Physiol 306:L299–L308

Green DE, Murphy TC, Kang BY, Kleinhenz JM, Szyndralewiez C, Page P, Sutliff RL, Hart CM (2012) The Nox4 inhibitor GKT137831 attenuates hypoxia-induced pulmonary vascular cell proliferation. Am J Respir Cell Mol Biol 47:718–726

Guignabert C, Alvira CM, Alastalo TP, Sawada H, Hansmann G, Zhao M, Wang L, El-Bizri N, Rabinovitch M (2009) Tie2-mediated loss of peroxisome proliferator-activated receptor-gamma in mice causes PDGF receptor-beta-dependent pulmonary arterial muscularization. Am J Physiol Lung Cell Mol Physiol 297:L1082–L1090

Han X, Chen C, Cheng G, Liang L, Yao X, Yang G, You P, Shou X (2015) Peroxisome proliferator-activated receptor gamma attenuates serotonin-induced pulmonary artery smooth muscle cell proliferation and apoptosis inhibition involving ERK1/2 pathway. Microvasc Res 100:17–24

Hansmann G, de Jesus Perez VA, Alastalo TP, Alvira CM, Guignabert C, Bekker JM, Schellong S, Urashima T, Wang L, Morrell NW, Rabinovitch M (2008) An antiproliferative BMP-2/PPARgamma/apoE axis in human and murine SMCs and its role in pulmonary hypertension. J Clin Invest 118:1846–1857

Hosokawa S, Haraguchi G, Sasaki A, Arai H, Muto S, Itai A, Doi S, Mizutani S, Isobe M (2013) Pathophysiological roles of nuclear factor kappaB (NF-kB) in pulmonary arterial hypertension: effects of synthetic selective NF-kB inhibitor IMD-0354. Cardiovasc Res 99:35–43

Huang J, Kaminski PM, Edwards JG, Yeh A, Wolin MS, Frishman WH, Gewitz MH, Mathew R (2008) Pyrrolidine dithiocarbamate restores endothelial cell membrane integrity and attenuates monocrotaline-induced pulmonary artery hypertension. Am J Physiol Lung Cell Mol Physiol 294:L1250–L1259

Humbert M, Sitbon O, Chaouat A, Bertocchi M, Habib G, Gressin V, Yaici A, Weitzenblum E, Cordier JF, Chabot F, Dromer C, Pison C, Reynaud-Gaubert M, Haloun A, Laurent M, Hachulla E, Cottin V, Degano B, Jais X, Montani D, Souza R, Simonneau G (2010) Survival in patients with idiopathic, familial, and anorexigen-associated pulmonary arterial hypertension in the modern management era. Circulation 122:156–163

Humbert M, Sitbon O, Simonneau G (2004) Treatment of pulmonary arterial hypertension. N Engl J Med 351:1425–1436

Jennewein C, von Knethen A, Schmid T, Brune B (2010) MicroRNA-27b contributes to lipopolysaccharide-mediated peroxisome proliferator-activated receptor gamma (PPARgamma) mRNA destabilization. J Biol Chem 285:11846–11853

Jin D, Tao J, Li D, Wang Y, Li L, Hu Z, Zhou Z, Chang X, Qu C, Zhang H (2015a) Golgi protein 73 activation of MMP-13 promotes hepatocellular carcinoma cell invasion. Oncotarget 6:33523–33533

Jin H, Gebska MA, Blokhin IO, Wilson KM, Ketsawatsomkron P, Chauhan AK, Keen HL, Sigmund CD, Lentz SR (2015b) Endothelial PPAR-gamma protects against vascular thrombosis by downregulating P-selectin expression. Arterioscler Thromb Vasc Biol 35:838–844

Kang BY, Park KK, Green DE, Bijli KM, Searles CD, Sutliff RL, Hart CM (2013) Hypoxia mediates mutual repression between microRNA-27a and PPARgamma in the pulmonary vasculature. PLoS ONE 8:e79503

Ke R, Liu L, Zhu Y, Li S, Xie X, Li F, Song Y, Yang L, Gao L, Li M (2016) Knockdown of AMPKalpha2 promotes pulmonary arterial smooth muscle cells proliferation via mTOR/Skp2/p27(Kip1) signaling pathway. Int J Mol Sci 17:844

Keller RL, Tacy TA, Hendricks-Munoz K, Xu J, Moon-Grady AJ, Neuhaus J, Moore P, Nobuhara KK, Hawgood S, Fineman JR (2010) Congenital diaphragmatic hernia: endothelin-1, pulmonary hypertension, and disease severity. Am J Respir Crit Care Med 182: 555–561

Kelly D, Campbell JI, King TP, Grant G, Jansson EA, Coutts AG, Pettersson S, Conway S (2004) Commensal anaerobic gut bacteria

attenuate inflammation by regulating nuclear-cytoplasmic shuttling of PPAR-gamma and RelA. Nat Immunol 5:104–112

Kim EK, Lee JH, Oh YM, Lee YS, Lee SD (2010a) Rosiglitazone attenuates hypoxia-induced pulmonary arterial hypertension in rats. Respirology 15:659–668

Kim SY, Kim AY, Lee HW, Son YH, Lee GY, Lee JW, Lee YS, Kim JB (2010b) miR-27a is a negative regulator of adipocyte differentiation via suppressing PPARgamma expression. Biochem Biophys Res Commun 392:323–328

Kojonazarov B, Isakova J, Imanov B, Sovkhozova N, Sooronbaev T, Ishizaki T, Aldashev AA (2012) Bosentan reduces pulmonary artery pressure in high altitude residents. High Altitude Med Biol 13:217–223

Kollipara RK, Kittler R (2015) An integrated functional genomic analysis identifies the antitumorigenic mechanism of action for PPARgamma in lung cancer cells. Genom Data 3:80–86

Kwon YS, Chi SY, Shin HJ, Kim EY, Yoon BK, Ban HJ, Oh IJ, Kim KS, Kim YC, Lim SC (2010) Plasma C-reactive protein and endothelin-1 level in patients with chronic obstructive pulmonary disease and pulmonary hypertension. J Korean Med Sci 25:1487–1491

Li L, Wei C, Kim IK, Janssen-Heininger Y, Gupta S (2014) Inhibition of nuclear factor-kappaB in the lungs prevents monocrotaline-induced pulmonary hypertension in mice. Hypertension 63:1260–1269

Li M, Li Z, Sun X, Yang L, Fang P, Liu Y, Li W, Xu J, Lu J, Xie M, Zhang D (2010) Heme oxygenase-1/p21WAF1 mediates peroxisome proliferator-activated receptor-gamma signaling inhibition of proliferation of rat pulmonary artery smooth muscle cells. FEBS J 277:1543–1550

Li S, Li J, Fei BY, Shao D, Pan Y, Mo ZH, Sun BZ, Zhang D, Zheng X, Zhang M, Zhang XW, Chen L (2015) MiR-27a promotes hepatocellular carcinoma cell proliferation through suppression of its target Gene peroxisome proliferator-activated receptor gamma. Chin Med J 128:941–947

Lin Q, Gao Z, Alarcon RM, Ye J, Yun Z (2009) A role of miR-27 in the regulation of adipogenesis. FEBS J 276:2348–2358

Liu S, Yang Y, Wu J (2011) TNFalpha-induced up-regulation of miR-155 inhibits adipogenesis by down-regulating early adipogenic transcription factors. Biochem Biophys Res Commun 414:618–624

Liu T, Tang H, Lang Y, Liu M, Li X (2009) MicroRNA-27a functions as an oncogene in gastric adenocarcinoma by targeting prohibitin. Cancer Lett 273:233–242

Liu Y, Tian XY, Huang Y, Wang N (2014) Rosiglitazone attenuated endothelin-1-induced vasoconstriction of pulmonary arteries in the rat model of pulmonary arterial hypertension via differential regulation of ET-1 receptors. PPAR Res 2014:374075

Liu Y, Tian XY, Mao G, Fang X, Fung ML, Shyy JY, Huang Y, Wang N (2012) Peroxisome proliferator-activated receptor-gamma ameliorates pulmonary arterial hypertension by inhibiting 5-hydroxytryptamine 2B receptor. Hypertension 60:1471–1478

Livak KJ, Schmittgen TD (2001) Analysis of relative gene expression data using real-time quantitative PCR and the 2(−Delta Delta C(T)) method. Methods 25:402–408

Lu X, Bijli KM, Ramirez A, Murphy TC, Kleinhenz J, Hart CM (2013) Hypoxia downregulates PPARgamma via an ERK1/2-NF-kappaB-Nox4-dependent mechanism in human pulmonary artery smooth muscle cells. Free Radic Biol Med 63:151–160

Lu X, Murphy TC, Nanes MS, Hart CM (2010) PPAR{gamma} regulates hypoxia-induced Nox4 expression in human pulmonary artery smooth muscle cells through NF-{kappa}B. Am J Physiol Lung Cell Mol Physiol 299:L559–L566

Luo S, Wang J, Ma Y, Yao Z, Pan H (2015) PPARgamma inhibits ovarian cancer cells proliferation through upregulation of miR-125b. Biochem Biophys Res Commun 462:85–90

Lv J, Qiu M, Xia W, Liu C, Xu Y, Wang J, Leng X, Huang S, Zhu R, Zhao M, Ji F, Xu L, Xu K, Yin R (2016) High expression of long non-coding RNA SBF2-AS1 promotes proliferation in non-small cell lung cancer. J Exp Clin Cancer Res: CR 35:75

Mansure JJ, Nassim R, Chevalier S, Szymanski K, Rocha J, Aldousari S, Kassouf W (2013) A novel mechanism of PPAR gamma induction via EGFR signalling constitutes rational for combination therapy in bladder cancer. PLoS ONE 8:e55997

Matsuda Y, Hoshikawa Y, Ameshima S, Suzuki S, Okada Y, Tabata T, Sugawara T, Matsumura Y, Kondo T (2005) Effects of peroxisome proliferator-activated receptor gamma ligands on monocrotaline-induced pulmonary hypertension in rats. Nihon Kokyuki Gakkai Zasshi 43:283–288

Milenkovic D (2014) MicroRNAs as novel nutrigenomic targets for cardiovascular health. Free Radic Biol Med 75(Suppl 1):S11

Monaco C, Andreakos E, Kiriakidis S, Mauri C, Bicknell C, Foxwell B, Cheshire N, Paleolog E, Feldmann M (2004) Canonical pathway of nuclear factor kappa B activation selectively regulates proinflammatory and prothrombotic responses in human atherosclerosis. Proc Natl Acad Sci U S A 101:5634–5639

Pellerito O, Notaro A, Sabella S, De Blasio A, Vento R, Calvaruso G, Giuliano M (2014) WIN induces apoptotic cell death in human colon cancer cells through a block of autophagic flux dependent on PPARgamma down-regulation. Apoptosis 19:1029–1042

Rahman A, Fazal F (2011) Blocking NF-kappaB: an inflammatory issue. Proc Am Thorac Soc 8:497–503

Sawada H, Mitani Y, Maruyama J, Jiang BH, Ikeyama Y, Dida FA, Yamamoto H, Imanaka-Yoshida K, Shimpo H, Mizoguchi A, Maruyama K, Komada Y (2007) A nuclear factor-kappaB inhibitor pyrrolidine dithiocarbamate ameliorates pulmonary hypertension in rats. Chest 132:1265–1274

Song Y, Wu Y, Su X, Zhu Y, Liu L, Pan Y, Zhu B, Yang L, Gao L, Li M (2016) Activation of AMPK inhibits PDGF-induced pulmonary arterial smooth muscle cells proliferation and its potential mechanisms. Pharmacol Res 107:117–124

Stewart DJ, Levy RD, Cernacek P, Langleben D (1991) Increased plasma endothelin-1 in pulmonary hypertension: marker or mediator of disease? Ann Intern Med 114:464–469

Wolf D, Tseng N, Seedorf G, Roe G, Abman SH, Gien J (2014) Endothelin-1 decreases endothelial PPARgamma signaling and impairs angiogenesis after chronic intrauterine pulmonary hypertension. Am J Physiol Lung Cell Mol Physiol 306:L361–L371

Wu Y, Liu L, Zhang Y, Wang G, Han D, Ke R, Li S, Feng W, Li M (2014) Activation of AMPK inhibits pulmonary arterial smooth muscle cells proliferation. Exp Lung Res 40:251–258

Xie X, Wang G, Zhang D, Zhang Y, Zhu Y, Li F, Li S, Li M (2015) Activation of peroxisome proliferator-activated receptor gamma ameliorates monocrotaline-induced pulmonary arterial hypertension in rats. Biomed Rep 3:537–542

Xing Y, Zheng X, Li G, Liao L, Cao W, Xing H, Shen T, Sun L, Yang B, Zhu D (2015) MicroRNA-30c contributes to the development of hypoxia pulmonary hypertension by inhibiting platelet-derived growth factor receptor beta expression. Int J Biochem Cell Biol 64:155–166

Yang S, Banerjee S, Freitas A, Cui H, Xie N, Abraham E, Liu G (2012) miR-21 regulates chronic hypoxia-induced pulmonary vascular remodeling. Am J Physiol Lung Cell Mol Physiol 302:L521–L529

Yuan P, Wu WH, Gao L, Zheng ZQ, Liu D, Mei HY, Zhang ZL, Jing ZC (2013) Oestradiol ameliorates monocrotaline pulmonary hypertension via NO, prostacyclin and endothelin-1 pathways. Eur Respir J 41:1116–1125

Zeng Y, Liu H, Kang K, Wang Z, Hui G, Zhang X, Zhong J, Peng W, Ramchandran R, Raj JU, Gou D (2015) Hypoxia inducible factor-1 mediates expression of miR-322: potential role in proliferation and migration of pulmonary arterial smooth muscle cells. Sci Rep 5: 12098

Zhang D, Wang G, Han D, Zhang Y, Xu J, Lu J, Li S, Xie X, Liu L, Dong L, Li M (2014) Activation of PPAR-gamma ameliorates pulmonary arterial hypertension via inducing heme oxygenase-1 and p21(WAF1): an in vivo study in rats. Life Sci 98:39–43

Zhang S, Liu F, Mao X, Huang J, Yang J, Yin X, Wu L, Zheng L, Wang Q (2015) Elevation of miR-27b by HPV16 E7 inhibits PPARgamma expression and promotes proliferation and invasion in cervical carcinoma cells. Int J Oncol 47:1759–1766

Zhang TT, Cui B, Dai DZ, Su W (2005) CPU 86017, p-chlorobenzyltetrahydroberberine chloride, attenuates monocrotaline-induced pulmonary hypertension by suppressing endothelin pathway. Acta Pharmacol Sin 26: 1309–1316

Zhu H, Wu H, Liu X, Evans BR, Medina DJ, Liu CG, Yang JM (2008) Role of MicroRNA miR-27a and miR-451 in the regulation of MDR1/P-glycoprotein expression in human cancer cells. Biochem Pharmacol 76:582–588

Zhu Y, Zhang X, Ding X, Wang H, Chen X, Zhao H, Jia Y, Liu S, Liu Y (2014) miR-27 inhibits adipocyte differentiation via suppressing CREB expression. Acta Biochim Biophys Sin 46:590–596